

DGI: EASY AND EFFICIENT INFERENCE FOR GNNs

Peiqi Yin^{1,2,3} Xiao Yan³ Jinjing Zhou⁴ Qiang Fu⁵ Zhenkun Cai¹ James Cheng² Bo Tang³ Minjie Wang¹

ABSTRACT

While many systems have been developed to train Graph Neural Networks (GNNs), efficient model inference and evaluation remain to be addressed. For instance, using the widely adopted *node-wise* approach, model evaluation can account for up to 94% of the time in the end-to-end training process due to *neighbor explosion*, which means that a node accesses its multi-hop neighbors. On the other hand, *layer-wise* inference avoids the neighbor explosion problem by conducting inference layer by layer such that the nodes only need their one-hop neighbors in each layer. However, implementing layer-wise inference requires substantial engineering efforts because users need to manually decompose a GNN model into layers for computation and split workload into batches to fit into device memory. In this paper, we develop *Deep Graph Inference (DGI)* — a system for easy and efficient GNN model inference, which automatically translates the training code of a GNN model for layer-wise execution. DGI is general for various GNN models and different kinds of inference requests, and supports out-of-core execution on large graphs that cannot fit in CPU memory. Experimental results show that DGI consistently outperforms layer-wise inference across different datasets and hardware settings, and the speedup can be over 1,000x.

1 INTRODUCTION

Graph data are ubiquitous in domains such as social networks (Mandal & Maiti, 2021; Wang et al., 2018), knowledge representations (Hamaguchi et al., 2017), and bioinformatics (Gaudeflet et al., 2021; Cheung & Moura, 2020). Recently, graph neural networks (GNNs) have shown outstanding performance for many tasks including node classification (Garcia Duran & Niepert, 2017; Hu et al., 2020a), clustering (Riesen & Bunke, 2010), and link prediction (Kunegis & Lommatzsch, 2009; Zhang & Chen, 2018). A plethora of GNN models with different structures have been proposed, e.g., GCN (Kipf & Welling, 2017), GAT (Veličković et al., 2018), JKNet (Xu et al., 2018) and APPNP (Klicpera et al., 2018). These models generally stack L graph aggregation (also called convolution) layers to compute an output embedding h_v^L for each node v in a graph $G = (V, E)$, and each layer can be expressed as

$$h_v^l = \text{AGGREGATE}^l(h_u^{l-1}, \forall u \in \mathcal{N}(v) \cup v; w^l), \quad (1)$$

where set $\mathcal{N}(v)$ contains the in-neighbors of node v , h_v^l is the embedding of node v in the l^{th} layer (with h_v^0 being the input node embedding), and w^l is the parameter of function AGGREGATE^l .

GNN inference computes output embeddings for all (or a

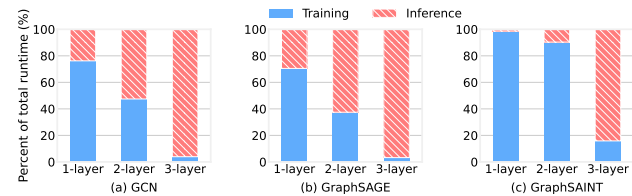


Figure 1. Composition of model training time and node-wise inference time in a model training pipeline for the *OGBN-Products* graph on a V100 GPU with 32GB memory. All experiments conduct evaluation every 10 training epochs following the setting of models in OGB Leaderboard (Hu et al., 2020a).

set of) nodes in the graph to facilitate model evaluation or downstream applications (e.g., recommendation). A natural solution is to utilize the code for training, which usually computes output embedding for each target node v individually by first collecting its L -hop neighbors and then applying Eq. (1). We call this approach *node-wise inference* and report the time taken by model training and inference (evaluation) for some popular GNNs in Figure 1. The results show that inference time increases quickly with the number of layers and accounts for up to 94% of the end-to-end time. This is because node-wise inference suffers from *neighbor explosion*: (i) The L -hop neighbors of a target node and the input embeddings of these neighbors are enormous, which make data preparation expensive. (ii) To fit the memory of GPU, inference is normally conducted in small batch. Target nodes in different batches compute intermediate embeddings (i.e., in layers with $l < L$) for their common neighbors, resulting in repetitive computation.

¹AWS Shanghai AI Lab ²The Chinese University of Hong Kong
³Southern University of Science and Technology ⁴TensorChord
⁵The George Washington University. Correspondence to: Minjie Wang <minjiw@amazon.com>.

The neighbor explosion problem is prominent for inference because (i) it usually uses the full neighborhood as opposed to the neighbor sampling in training (Hamilton et al., 2017; Chen et al., 2018; Chiang et al., 2019), and (ii) real-world graphs contain popular nodes with a large number of neighbors, and thus the size of L -hop neighborhood could be very large (Hu et al., 2020a; Yang & Leskovec, 2015).

We present an efficient *layer-wise inference* approach, which conducts computation layer by layer and handles the tasks of all target nodes in the same layer batch by batch. Layer-wise inference avoids the neighbor explosion problem as a node only accesses its 1-hop neighbors in each layer. The small input set also enables efficient out-of-core execution for large graphs by storing data in external memory and loading only the input set of each batch. Moreover, common computation tasks in a layer from different target nodes are merged to eliminate repetitive computation. However, substantial implementation efforts are required to enjoy the efficiency of layer-wise inference. In particular, users need to manually decompose a GNN model into layers, merge the computation tasks in each layer, and manage the intermediate embeddings and node batching. Figures 2(b-c) show that GNN models can be much more complex than the linear structure in Figure 2(a), and thus it is difficult to decompose them into layers that are suitable for inference. Moreover, the batch size is cumbersome to set in order to fully utilize memory while avoiding out-of-memory (OOM).

To mitigate the programming difficulty of layer-wise inference, we build *Deep Graph Inference (DGI)* — a system for easy and efficient GNN inference. DGI generalizes across GNN models (e.g., homogeneous and heterogeneous ones) and automatically translates the training code for layer-wise execution, and thus removes the burden of writing separate code for inference. In particular, DGI uses a tracer to resolve the computation graph of a GNN model, designs tailored rules to partition the computation graph into layers, and schedules the layers for computation. DGI also dynamically adjusts the batch size according to runtime statistics and reorders the graph nodes to form batches for better input sharing in each batch. DGI can handle different kinds of inference requests: (i) *full inference*, which computes output embedding for all nodes in the graph, (ii) *partial inference*, which computes output embedding for a set of nodes, and (iii) *sampling inference*, which samples neighborhood during inference (as in training) to trade accuracy for efficiency. DGI also supports out-of-core execution for large graphs. Users can enjoy the efficiency of layer-wise inference and all these functionalities via simple configurations.

We evaluate DGI on 6 real graphs, 5 GNN models with different structures, and various hardware configurations. The results show that DGI consistently outperforms node-wise inference across different settings, and the speedup of

DGI over node-wise inference can be up to 1,000x and is usually 10x-100x. Experiments also show that DGI handles different kinds of inference requests efficiently and its inference time scales linearly with the number of layers. Micro experiments show that dynamic batch size control and node reordering are effective in reducing inference time.

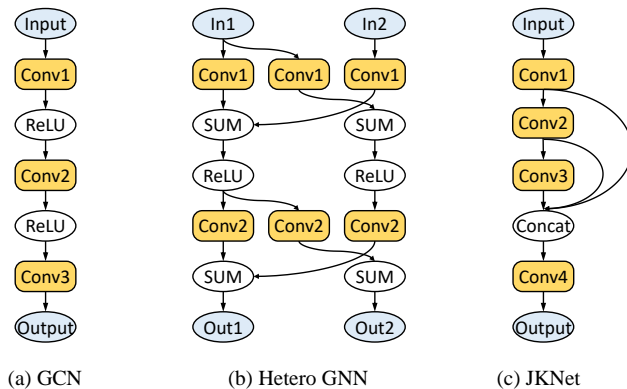


Figure 2. The structure of different GNN models. Conv is a graph aggregation layer, and we omit the activation functions in (c).

2 LAYER-WISE INFERENCE APPROACH

Given a graph $G = (V, E)$ and the input (i.e., layer-0) embedding of all nodes \mathcal{H}^0 , GNN inference computes output embedding using an L -layer GNN model. Algorithm 1 is the pseudo-code of node-wise inference, and Figure 3(b) provides a running example. In Algorithm 1, set \mathcal{N}_v^L contains all L -hop neighbors of node v , and $\mathcal{H}^0(\mathcal{N}_v^L)$ indicates the input embedding of these neighbors. We assume that input data is stored on an external device (e.g., CPU) and fetched to the computing device (e.g., GPU) for execution in batches. In a batch, node-wise inference takes three steps, i.e., data preparation (Lines 4-6 in Algorithm 1), data transfer (Lines 7 and 9), and computation (Line 8).

For data preparation, a target node v accesses all its L -hop neighbors, which results in a large input set (i.e., neighbor explosion) as the number of neighbors increases quickly with layers. In particular, for super nodes, which have many neighbors and are common in real-world graphs, the input set can constitute a large portion of the entire graph. For this reason, we observe that even with a batch size of 1, node-wise inference can run OOM on GPU for processing large graphs. Regarding computation, each batch of target nodes is handled independently, and thus different target nodes conduct repetitive computation for their common neighbors. For the example in Figure 3(b), computing the layer-2 embeddings of both nodes A and B requires the layer-1 embeddings of nodes C and D, and thus the layer-1 embeddings of nodes C and D are computed twice. Empirically, the running time of node-wise inference increases

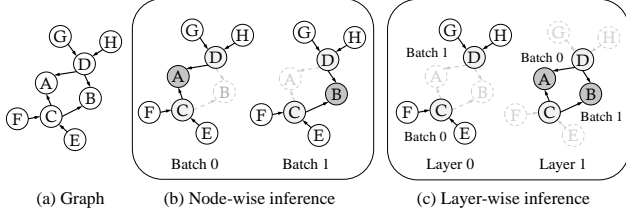


Figure 3. Node-wise and layer-wise inference for a 2-layer GNN model on a toy graph. Both examples illustrate the process to compute output embeddings for node A and B, in two batches with a batch size of 1.

exponentially with the number of layers and constitutes a major part of the training pipeline for multi-layer models.

Algorithm 1 Node-wise Inference for an L -layer GNN

```

1:  $\mathcal{H}^L \leftarrow$  empty tensor for holding output embedding
2: for each batch  $V_B$  of nodes in  $V$  do
3:    $\mathcal{N} \leftarrow$  null neighbor set,  $\mathcal{H} \leftarrow$  null input embedding set
4:   for each node  $v$  in  $V_B$  do
5:      $\mathcal{N} = \mathcal{N} \cup \mathcal{N}_v^L$ ,  $\mathcal{H} = \mathcal{H} \cup \mathcal{H}^0(\mathcal{N}_v^L)$ 
6:   end for
7:   Copy  $\mathcal{N}$  and  $\mathcal{H}$  to the computing device
8:   Run Eq. (1) for each node  $v$  in  $V_B$  to obtain  $\mathcal{H}^L(V_B)$ 
9:   Store  $\mathcal{H}^L(V_B)$  to back to  $\mathcal{H}^L$ 
10: end for
    
```

Algorithm 2 Layer-wise Inference for an L -layer GNN

```

1: for layer  $l \in \{1, 2, \dots, L\}$  do
2:    $\mathcal{H}^l \leftarrow$  empty tensor for layer- $l$  embedding
3:   for each batch  $V_B$  of nodes in  $V$  do
4:      $\mathcal{N} \leftarrow$  null neighbor set,  $\mathcal{H} \leftarrow$  null input embedding set
5:     for each node  $v \in V_B$  do
6:        $\mathcal{N} = \mathcal{N} \cup \mathcal{N}_v$ ,  $\mathcal{H} = \mathcal{H} \cup \mathcal{H}^{l-1}(\mathcal{N}_v)$ 
7:     end for
8:     Copy  $\mathcal{N}$  and  $\mathcal{H}$  to the computing device
9:     Run layer- $l$  of Eq. (1) and get the output  $\mathcal{H}^l(V_B)$ 
10:    Store  $\mathcal{H}^l(V_B)$  (layer- $l$  embedding of batch  $V_B$ ) into  $\mathcal{H}^l$ 
11:   end for
12:   Release storage for  $\mathcal{H}^{l-1}$  if it is no longer needed
13: end for
    
```

Algorithm 2 is the pseudo-code for layer-wise inference, and Figure 3(c) shows a running example. In Algorithm 2, \mathcal{H}^l contains the layer- l embedding for all nodes, and set \mathcal{N}_v is the 1-hop neighbors of node v . Algorithm 2 shows that layer-wise inference conducts computation layer by layer, which differs from the node by node scheme of node-wise inference. One advantage of layer-wise inference is small input set as each node only requires its 1-hop neighbors in data preparation (Line 6 of Algorithm 2). The small input set makes layer-wise inference less likely to run OOM for super nodes. Also, small input set allows a large batch size in the inner loop (Line 3 of Algorithm 2), which enables

good input sharing. For the example in Figure 3(c), if the layer-2 embedding of nodes A and B are computed in a batch, then the layer-1 embedding of nodes C and D are loaded to GPU only once and shared by nodes A and B. Another advantage of layer-wise inference is that it completely eliminates repetitive computation. For the example in Figure 3(c), both nodes A and B require the layer-1 embedding of nodes C and D, which are computed only once in layer-1.

We note that layer-wise and node-wise inference are equivalent in semantics because they produce the same output embedding. In Algorithm 2, we present layer-wise inference for full inference, which computes output embedding for all graph nodes without neighbor sampling and is a major use case (e.g., using GNN-generated embedding for applications). Layer-wise inference can also handle other kinds of inference requests. In particular, partial inference computes output embedding for only a subset of the graph nodes and can be used for model evaluation when only some nodes are associated with labels. Here we can conduct BFS of depth L from the target nodes to mark a node set V^l , which contains the nodes for which layer- l embeddings need to be computed. Algorithm 2 only needs to change the node set from V to V^l in Line 3. Instead of using all neighbors for each node, sampling inference selects some neighbors for aggregation, which is useful when users want to trade accuracy for efficiency. In this case, we mark the node set V^l according to the sampled 1-hop neighbors.

Although layer-wise inference has appealing advantages, a drawback is its programming difficulty. Firstly, node-wise inference can directly utilize the training code, while layer-wise inference requires to write separate code for inference. Secondly and more importantly, it can be difficult to decompose a GNN model into layers for inference when it goes beyond a linear stack of layers. For the examples in Figures 2(b) and (c), heterogeneous GNN models have complex connections among the normal operators and graph convolutions, while JKNet has jumping links that connect multiple graph convolution layers. In these cases, a programmer needs to determine a layer partition that is efficient for inference and manage the dependencies of the intermediate embeddings. We show an example in the Appendix for JKNet, whose forward code has only 8 LOCs, but layer-wise inference code needs more than 30 LOCs even after removing some API calls. Additional programming difficulties include: (i) managing the batch size to fit the memory of the computing device, (ii) handling out-of-core execution for large graphs stored on disk, and (iii) collecting the inference tasks in each layer for partial and sampling inference. These programming difficulties will be more prominent for future GNN models that are more complex (Wei et al., 2022).

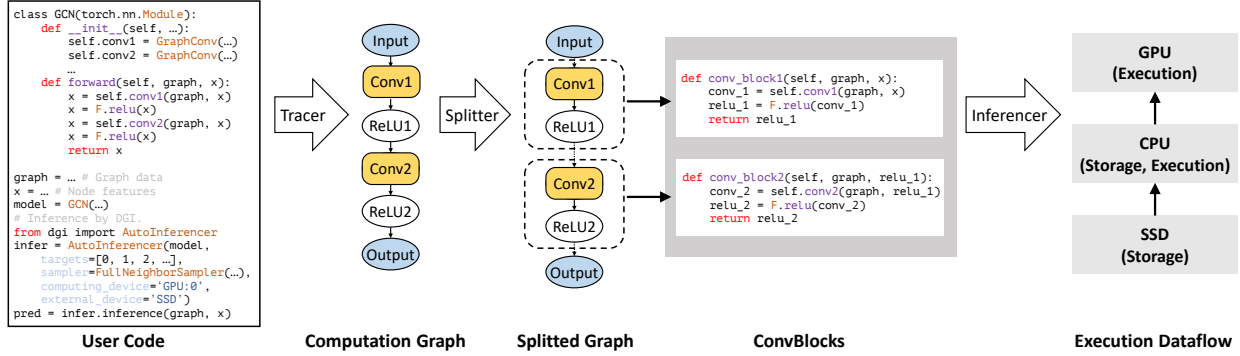


Figure 4. The workflow of DGI.

3 THE DGI SYSTEM

API and Overview. DGI is developed to make the use of layer-wise inference easy by automatically translating the training code for execution. We show an example of using DGI in the left part of Figure 4. Programmers first import the *AutoInferencer* class from the *dgi* library, and then use the (training code of the) GNN model to initialize an *AutoInferencer* object. Parameters to specify include the target nodes that need to compute output embedding (for partial inference, set as all nodes in the graph by default), the neighbor sampling strategy (for sampling inference, use all neighbors by default), the computing device (e.g., a GPU), and where to store the output tensors (e.g., CPU memory and SSD). Then the path of the graph data and input node embedding (i.e., graph and x) are fed to the *AutoInferencer* to conduct inference. The output embeddings are stored in *pred*. By default, DGI uses a single GPU for inference, and stores data in CPU memory.

DGI consists of three key modules, i.e., *tracer*, *splitter*, and *inferencer*, as shown in Figure 4. The tracer traces the python code of the GNN model and converts it into a computation graph, which consists of operators such as graph aggregation (denoted as Conv) and activation function. The splitter uses customized rules to partition the computation graph into *ConvBlocks*, with each ConvBlock corresponding to one layer of the GNN model. The tracer generates codes for executing each of those ConvBlocks. The splitter also generates a schema describing the dependencies of the ConvBlocks (i.e., a ConvBlock takes input from which ConvBlocks). The inferencer executes the ConvBlocks sequentially (i.e., layer by layer) and runs each ConvBlock in batches. For each batch, the target nodes and their 1-hop neighbors are collected for data preparation, then the batch is transferred to the GPU for computation, and finally the output embeddings of the target nodes are dumped to the CPU. DGI can be configured to fetch data from and store output embedding in SSD when CPU memory is not sufficient.

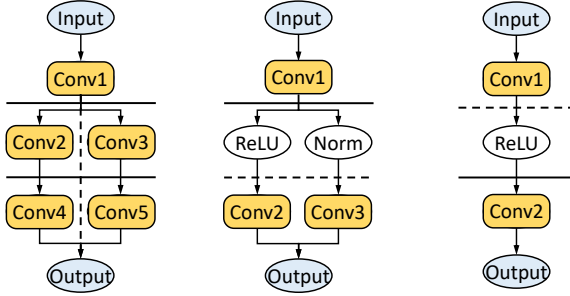
3.1 Tracer

The tracer converts the training code of a GNN model into a computation graph. We implement DGI tracer using Torch.fx as it generates computation graph in Python format. In particular, Torch.fx uses placeholders called *proxies* to replace the actual tensors and records the operators encountered by the proxies in the forward pass of a model. The resultant computation graph is a DAG, where nodes are operators and edges are the dependencies between operators. We classify the operators into two categories, i.e., *normal operator* and *graph convolution operator* (Conv for short). Normal operators work on the tensor of each individual graph node/edge, and examples include Add, ReLU, and MatMul. A Conv aggregates the 1-hop neighbors of a graph node to update its embedding. During tracing, DGI tracer recognizes the Conv operators by matching computation pattern. To allow the splitter to determine the execution order of the Conv operators, we associate an integer l to each Conv operator to indicate the layer it belongs to. In particular, we traverse the computation graph from the input, and mark the Conv operators that have no preceding Conv operators as layer 1. For a Conv operator with preceding Conv operators (called precursors), its layer is marked as one plus the maximum layer of its precursors.

3.2 Splitter

The DGI splitter partitions the computation graph of a GNN model into sub-graphs, and each sub-graph is treated as a ConvBlock (i.e., layer). We adopt the following three rules for computation graph partitioning.

Layer indexing. It means that Conv operators are organized into the same ConvBlock if and only if they have the same layer counter l . One such example is shown in Figure 5(a), where Conv2 and Conv3 are in the same ConvBlock because their layer counters are both 2. As the Conv operators in a ConvBlock have the same layer counter, the layer indexing rule ensures that a target node only needs its 1-hop neighbor nodes to execute each ConvBlock. An alternative is to treat



(a) Layer Indexing (b) Minimum Input (c) Upstream Binding

Figure 5. Illustrations of the rules for computation graph partitioning. The solid line denotes the partitioning adopted by DGI while the dotted line is an inferior alternative.

each Conv operator as a ConvBlock (which also satisfies layer-wise inference), for example, Conv2 and Conv3 could be two ConvBlocks. However, this partitioning misses possible opportunities for *input sharing* among ConvBlocks. For the example in Figure 5(a), both Conv2 and Conv3 take the output embedding of Conv1 as input, and thus can share input embeddings when they are loaded to the GPU. When treated as two separate ConvBlocks, Conv2 and Conv3 need to load the embedding generated by Conv1 individually.

Minimum input. It means that when there are multiple ways to partition two consecutive ConvBlocks, choose the way that yields the minimum number of input tensors for the downstream ConvBlock. Note that when an edge in the computation graph is selected as a cut, the output node embedding of the upstream ConvBlock is saved on the CPU and loaded to the GPU for the downstream ConvBlock. For the example in Figure 5(b), both the dotted line and the solid line satisfy the layer indexing rule. We choose the solid line as it only requires each neighbor node to transfer one embedding vector to the GPU for the second ConvBlock (by applying the ReLU and Norm operators to a node embedding after it is loaded to the GPU). In contrast, if the dotted line is used, each neighbor node needs to transfer two embedding vectors to the GPU (as ReLU and Norm are applied to the output of the upstream ConvBlock). Thus, the minimum input rule minimizes the neighbor node data required by each ConvBlock for small data transfer cost.

Upstream binding. It means that a normal operator should be grouped with the upstream ConvBlock when there are multiple partitioning schemes to minimize data transfer. For example, in Figure 5(c), we choose the solid line as the cut as it puts the ReLU operator in the first ConvBlock. This is because if we group normal operators with the downstream ConvBlock (i.e., using the dotted line), there will be repetitive computation. The reason is that a node usually serves as a neighbor node for multiple target nodes (e.g., node C is used by nodes A and B in Figure 3), and if the dotted line is

used, each target node needs to apply the normal operator on its neighbor nodes individually. In contrast, the solid line applies the normal operator only once for each neighbor node when generating output for the upstream ConvBlock. Thus, the upstream binding rule avoids repetitive computation.

Based on these rules, we adopt a 3-step procedure to partition the computation graph into ConvBlocks. First, we determine the ConvBlock of each Conv operator according to the layer counters of the Conv operators (i.e., layer indexing). Second, starting from the Conv operators of the same ConvBlock, we traverse their preceding operators in the computation graph to find the partition points with the minimum number of inputs (i.e., minimum input). If there are multiple minimum input points, we choose the one that groups the largest number of normal operators into the upstream ConvBlocks (i.e., upstream binding). Note that minimum input and upstream binding conflict sometimes (e.g., Figure 5(b)). We prioritize minimum input as repetitive data loading is more expensive than the repetitive execution of normal operators.

Given the partitioning results of the splitter, the tracer registers each ConvBlock to a python function for execution. As a ConvBlock may take input from multiple ConvBlocks (e.g., JKNet), we use a schema to record the dependencies among the ConvBlocks, and each ConvBlock fetches input embedding according to the schema. We store the output embedding of each ConvBlock in a separate map, and the output of a ConvBlock is deleted when there are no ConvBlocks depending on it.

3.3 Inferencer

The inferencer executes the ConvBlocks sequentially and runs each ConvBlock batch by batch. To execute a ConvBlock, the inferencer first allocates memory to hold its output node embeddings. For each batch, execution takes four steps: (i) *data preparation*, a set of target nodes V_B are selected for the batch, and for each node $v \in V_B$, its 1-hop in-neighbors are collected into the input set along with their embeddings (we modify DGL dataloader for this purpose); (ii) *data transfer*, input set of batch V_B is transferred to the GPU; (iii) *computation*, the output embeddings for nodes in V_B are computed on the GPU; and (iv) *embedding dumping*, the output embeddings are transferred back to CPU. To achieve a short inference time, the inferencer should execute each ConvBlock in a small number of batches while avoiding OOM, and we discuss node batching in Section 4.

For full inference, the target nodes of all ConvBlocks are the complete graph node set. For partial inference, the inferencer annotates the target nodes for each ConvBlock before execution. In particular, for an L -layer GNN model, the L^{th} layer target node set V^L contains the target nodes specified by the user. The $(L - 1)^{\text{th}}$ layer target node set V^{L-1}

contains the 1-hop in-neighbors of nodes in V^L . The annotation process goes on recursively until obtaining V^1 , which is the target node set for layer-1. For a ConvBlock on layer- l ($l \in [1, L]$), the inferencer only computes output embedding for nodes in V^l . Annotation is similar for sampling inference, where we annotate the sampled neighbors for nodes in V^{l+1} as V^l . We observe that the annotation process for V^l is expensive and the resultant target node sets contain most of the graph nodes if V^{l+1} ($l < L$) is already very large. As an optimization, we skip the annotation and directly assign all nodes to V^l when $|V^{l+1}| \times d_{avg} \geq n$, where d_{avg} is the average degree and n is the number of graph nodes.

4 HANDLE LARGE GRAPHS

Real-world graphs can be large and cause two problems for inference. First, for a layer, target nodes and input embedding may not fit in GPU memory, which requires to organize the target nodes into batches for computation and control the batch size. Second, graph data and intermediate embedding may not fit in CPU memory, which requires disk storage. We discuss related optimizations in this part.

4.1 Dynamic Batch Size Control

Batch size refers to the number of target nodes in a batch, and a good batch size should avoid exceeding GPU memory and be as large as possible. This is because a large batch size allows better input sharing (i.e., multiple target nodes share the same input node embedding) and thus reduces data transfer. However, determining a good batch size is challenging. First, it is difficult to estimate the memory consumption of neural network models due to reasons such as temporary tensors (Gao et al., 2020), and thus even experienced programmers can only choose a safe but small batch size before execution. Second, a static batch size may not be suitable for all batches. For example, if a batch mainly contains nodes with large in-degrees, a small batch size is needed when each target node has many neighbors while a large batch size should be used if a batch mainly contains nodes with small in-degrees.

Considering the challenges, we use a dynamic strategy to configure the batch size according to run-time statistics. In particular, we observe that the number of target nodes (i.e., batch size, denoted as n_t) and the total in-degrees of the target nodes (denoted as n_i) are closely related to the GPU memory consumption of a batch, and thus keep adding target nodes to a batch until either the node count threshold or edge count threshold is exceeded. The two thresholds are initialized as safe values to avoid OOM and adjusted in the inference process. Specifically, for the k^{th} batch, we measure its peak memory consumption as M_k , and adjust

the thresholds for the next batch as

$$r = M/M_k, \quad n_t^{k+1} = r \times n_t^k, \quad n_i^{k+1} = r \times n_i^k, \quad (2)$$

where n_t^k (resp. n_i^k) is the node count (resp. edge count) threshold for the k^{th} batch. M is the expected memory consumption and set as 90% of the available GPU memory. The rationale is to increase batch size if memory is underutilized. If a batch runs OOM, we reduce the thresholds to half of their previous values, and DGI re-conducts the batch. For quick node batching, we precompute prefix sum for the in-degrees of the nodes such that binary search can be used to find a batch of target nodes meeting the thresholds.

4.2 Node Reorder

A naive solution to node batching is to randomly group the target nodes into batches. This is sub-optimal as some target nodes can share input embedding to reduce data transfer. Take the graph in Figure 3 for example and consider a batch size of 2. If nodes A and C form a batch, 4 neighbor nodes are required (i.e., node A requires C and D, node C requires E and F); however, if nodes A and B form a batch, only 2 neighbor nodes are required as the in-neighbors of both A and B are C and D. Therefore, we should organize target nodes sharing common neighbors into the same batch. For this purpose, the natural solution is to partition the graph into strongly connected components and treat nodes in each component as a batch. However, graph partitioning tools such as METIS (Karypis & Kumar, 1997) and KaFFPaE (Sanders & Schulz, 2013) have long running time. Node reordering algorithms like Rabbit (Arai et al., 2016) and Gorder (?) run fast but are designed for improving cache hit and perform poorly for our purpose (see Section 5.3). Thus, we use a lightweight strategy to renumber the nodes and take nodes with consecutive ids as a batch. In particular, RCMK (Chan & George, 1980), a BFS-based algorithm, is used to enumerate the nodes, and ids are assigned to the nodes in their enumeration order. The rationale is that nodes adjacent in the BFS order are likely to share common neighbors.

4.3 SSD Support

DGI allows to store graph data and intermediate embeddings in SSD and automatically loads them to conduct inference. In particular, we use numpy (Harris et al., 2020) *memmap* to map SSD as part of CPU memory. A new graph type called *SSDGraph* is utilized to store the graph structure in CSC format on SSD, and an *SSDNeighborSampler* is developed to extract the adjacency lists of the target nodes from *SSDGraph* to CPU memory for each batch. The required input embeddings are also loaded to CPU memory using *memmap*. After the GPU finishes a batch, DGI writes the output embeddings back to SSD.

Table 1. Statistics of the graphs used in the experiments.

Name	Nodes	Edges	Input Dim.	Average Degree	Total Size
Livejournal1	4,847,571	86,220,856	100	17.8	2.45 GB
OGBN-Products	2,449,029	126,167,309	100	51.5	2.11 GB
OGBN-Papers100M	111,059,956	1,726,745,828	100	15.5	64.96 GB
Friendster	65,608,366	3,612,134,270	128	55.0	58.20 GB
OGBN-MAG (Hetero)	1,939,743	21,111,007	128	10.9	0.94 GB
OGBN-MAG240M (Hetero)	244,160,499	3,456,728,464	768	14.2	200.39 GB

Table 2. Execution time of node-wise inference and DGI (in seconds). For large datasets (*OGBN-Papers100M*, *Friendster* and *OGBN-MAG240M*), node-wise inference may encounter a super large input node set for 3-hop neighbors, which results in OOM. So here we use 2-layer GNN models for those large datasets. When node-wise inference runs for more than 10,000s, we estimate its execution time by $t \times \frac{1}{\alpha}$, where t is the elapsed execution time and α is the percentage of processed target nodes.

	OGBN-Products			Livejournal1			OGBN-MAG	
GNN Models (3 layers)	GCN	GAT	JKNet	GCN	GAT	JKNet	RGCN	HGT
Node-wise (V100-16GB)	7110	9740	7150	4330	5220	4890	208	263
DGI (V100-16GB)	6.08	8.96	6.70	11.0	16.9	13.5	19.7	22.0
Node-wise (V100-32GB)	1690	1970	1760	1630	2110	1990	143	204
DGI (V100-32GB)	4.51	6.09	4.20	6.32	10.5	7.10	12.8	14.9
	OGBN-Papers100M			Friendster			OGBN-MAG240M	
GNN Models (2 layers)	GCN	GAT	JKNet	GCN	GAT	JKNet	RGCN	HGT
Node-wise (V100-16GB)	3620	3980	3470	57300	81900	63700	29400	143000
DGI (V100-16GB)	370	607	343	425	741	435	999	1580
Node-wise (V100-32GB)	1950	3070	1940	48700	64900	33600	18200	70200
DGI (V100-32GB)	177	397	175	238	465	231	643	1010

5 EXPERIMENTAL EVALUATION

We introduce the experiment settings in Section 5.1, compare DGI with node-wise inference in Section 5.2, and evaluate the optimizations of DGI in Section 5.3.

5.1 Experiment Settings

We use 3 popular homogeneous GNN models, i.e., GCN (Kipf & Welling, 2017), GAT (Veličković et al., 2018), and JKNet (Xu et al., 2018), and 2 heterogeneous GNN models, i.e., RGCN (Schlichtkrull et al., 2018) and HGT (Hu et al., 2020b). GCN uses mean pooling to aggregate neighbor embeddings while GAT adopts multi-head attention (we use 2 attention heads). The final layer of JKNet aggregates neighbor embeddings from all preceding layers. Both RGCN and HGT work on heterogeneous graphs and aggregate neighbor embeddings based on certain *src-edge-dst* type triplets. For all models, the dimension of intermediate embedding is set as 128. We conduct experiments on 6 popular and public graphs, i.e., *OGBN-Products*, *OGBN-MAG*, *OGBN-Papers100M*, *OGBN-MAG240M* from the Open Graph Benchmark (Hu et al., 2020a), and *Friendster*, *Livejournal1* from the Stanford Network Analysis Platform (Yang & Leskovec, 2015). Table 1 reports the statistics of the graphs. Among them, *OGBN-MAG* and *OGBN-MAG240M* are heterogeneous graphs used to experiment heterogeneous GNNs.

Both DGI and the baselines are implemented on top of DGL. We use two different machines for the experiments. One machine has an Intel(R) Xeon(R) E5-2686 CPU with 96 cores, 488 GB main memory, and one NVIDIA V100 GPU with 16GB HBM (denoted as V100-16GB). The other machine has an Intel(R) Xeon(R) Gold 6126 CPU with 24 cores, 1.5TB main memory, and one NVIDIA V100 with 32GB GPU HBM (denoted as V100-32GB). The two machines have sufficient main memory to store data and intermediate embedding for all graphs, and we use them to explore the influence of GPU memory. We use the execution time of inference as the main performance metric and keep 3 effective numbers in the results. For partial inference, we randomly sample some nodes from the graph as the target nodes. For sampling inference, we use a fan-out of 10 for all layers following the GraphSage (Hamilton et al., 2017) implementation in DGL (Wang et al., 2019), which means that each target node samples 10 neighbors. To run node-wise inference, we use a grid search to find the batch size that minimizes inference time.

5.2 Main Results

Full inference. We report the execution time of node-wise inference and DGI for full inference in Table 2, which lead to several observations. Firstly, DGI consistently outperforms node-wise inference for all datasets, models and hardware configurations, and the speedup ranges from 10.6x

Table 3. Execution time of node-wise inference and DGI (in seconds) for full inference the changing the number of layers. The graph is *OGBN-Products*, “*” means that JKNet requires at least 2 layers, and "OOM" indicates that an out-of-memory exception was raised.

# of Layers	GCN				GAT				JKNet			
	1	2	3	4	1	2	3	4	1	2	3	4
Node-wise (V100-16GB)	3.16	153	7110	OOM	3.03	189	8740	OOM	*	152	7150	OOM
DGI (V100-16GB)	2.60	4.37	6.10	9.79	2.62	5.68	8.96	14.5	*	4.31	6.70	11.9
Node-wise (V100-32GB)	2.56	26.8	1690	69400	2.63	29.4	1970	122000	*	70.2	1760	90900
DGI (V100-32GB)	1.75	3.32	4.51	5.40	1.95	4.76	6.09	8.10	*	3.29	4.20	5.71

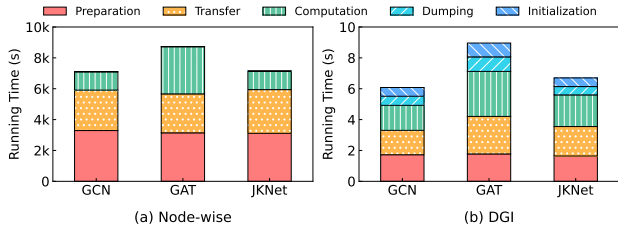


Figure 6. Decomposing the running time of node-wise inference and DGI for full inference. The results are obtained for the *OGBN-Products* graph on V100-16GB with 3-layer models.

to over 1000x. Considering the homogeneous GNNs (i.e., GCN, GAT and JKNet), DGI yields larger speedup for 3-layer models and dense graphs (i.e., having large average degrees). In particular, 3-layer models all observe over 2 orders of magnitude speedup while 2-layer models may have 10x speedups. For 2-layer models, the speedup of DGI is 10x for *OGBN-Papers100M* (with an average degree of 15.5) and 100x for *Friendster* (with an average degree of 55). This is because more layers and denser graphs make node-wise inference access more neighbor nodes for each target node, which aggravates the neighbor explosion problem. Secondly, both DGI and node-wise inference run faster on V100-32GB than V100-16GB because larger GPU memory allows larger batch size, and thus there are more opportunities for input sharing. Thirdly, DGI generally observes smaller speedups for the heterogeneous GNNs (i.e., RGCN and HGT) than the homogeneous GNNs. This is because each Conv only aggregates neighbors of a specific type in heterogeneous GNNs, and thus the neighbor explosion problem of node-wise inference is alleviated. Comparing the results on *OGBN-MAG* and *OGBN-MAG240M*, we also observe that DGI has larger speedup on bigger and denser graphs for heterogeneous GNNs.

In Table 3, we compare node-wise inference and DGI by changing the number of layers in the GNN models. The results show that the running time of node-wise inference increases quickly with the number of layers. This is because node-wise inference accesses L -hop neighbors for L -layer models, and the number of neighbors increases quickly with L . In contrast, the execution time of DGI increases almost linearly with the number of layers as layer-wise inference only accesses one-hop neighbors and is free from the neigh-

bor explosion problem. For 1-layer models, node-wise inference and the layer-wise inference of DGI are equivalent, and thus they yield comparable running time. For 4-layer models, DGI usually outperforms node-wise inference by more than 1000x, and node-wise inference easily goes OOM.

To understand the speedup of DGI over node-wise inference, we decompose their running time in Figure 6. The first 4 time consumptions are introduced in Section 3.3, and *initialization* means initializing dataloader and creating empty tensors for output embeddings. Notice that the y-axis uses different scales for DGI and node-wise inference. The results show that node-wise inference uses significantly longer time than DGI for data preparation, data transfer and GNN forward, which make the time for embedding dumping and initialization negligible. In particular, each of the three parts (i.e., preparation, data transfer and GNN forward) takes thousands of seconds for node-wise inference but only several seconds for DGI. This is because node-wise inference accesses L -hops neighbors for data preparation, and the large input set results in a small batch size, which makes input and computation sharing difficult. In contrast, data preparation is quick for DGI as it only accesses 1-hop neighbors, and small input set enables large batch size for good input sharing.

Partial inference. We compare node-wise inference and DGI for partial inference in Figure 7. The results show that when increasing the number of target nodes, the inference time increases linearly for node-wise inference but sub-linearly for DGI. This is because DGI effectively shares common computation and input nodes for different target nodes while sharing is difficult for node-wise inference due to the small batch size caused by neighbor explosion. While DGI and node-wise inference perform comparably when the target node set is small (e.g., 0.1% of all graph nodes), the speedup of DGI over node-wise inference increases with the number of target nodes. This is because more target nodes enables DGI to better share input and computation.

Sampling inference. Instead of using exact inference with the complete neighbor set, some users may use neighbour sampling for inference to trade accuracy for efficiency. We compare DGI and node-wise inference for sampling inference in Table 4. As sampling mitigates the neighbor explo-

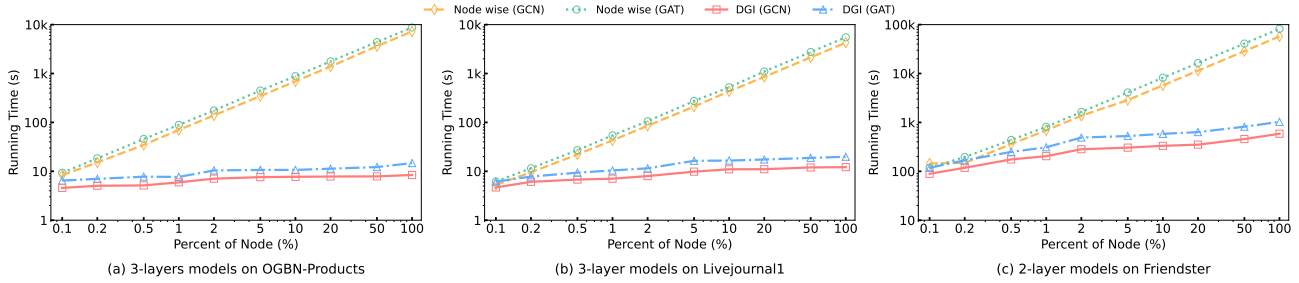


Figure 7. Running time of DGI and node-wise for partial inference (on V100-16GB GPU). Note that both axes use log scale.

Table 4. Running time (in seconds) of sampling-based inference for 3-layer GCN. We use aberrations for the 4 datasets, i.e., *OGBN-Products*, *Livejournal1*, *OGBN-Papers100M*, and *Friendster*.

	Prods	Livej1	Papers	Friend
Node-wise (16GB V100)	17.7	30.1	1390	3530
DGI (16GB V100)	4.97	7.92	341	166
Node-wise (32GB V100)	11.4	23.3	1149	1895
DGI (32GB V100)	3.13	5.43	166	121

sion problem of node-wise inference, it can handle 3-layer models on the large graphs (e.g., *Friendster*). However, the results show that DGI still consistently outperforms node-wise inference. In particular, the speedup of DGI is several times for the small graphs (i.e., *OGBN-Products* and *Livejournal1*) but becomes over 10x for the large graphs. This is because DGI only accesses 1-hop neighbors for each node and thus still achieves better input node and computation sharing than node-wise inference.

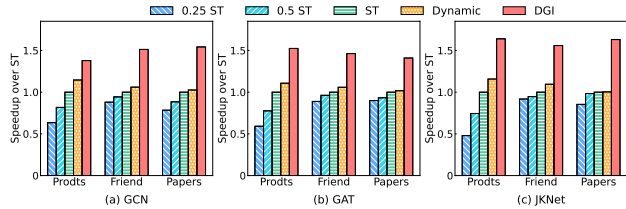


Figure 8. Effect of dynamic batch size and node ordering for 3-layer models on V100-16GB GPU. Inference time is reported as speedup over *ST*.

5.3 Micro Experiments

DGI comes with two key optimizations, i.e., node reordering and dynamic batch size control. To evaluate their effects, we design 4 baselines: *0.25ST*, *0.5ST*, *ST*, and *Dynamic*, which all adopt the layer-wise inference scheme. *ST* uses the best static batch size (found by grid search) that minimizes inference time. We also include *0.5ST* and *0.25ST*, which use 0.5 and 0.25 of the *ST* batch size, respectively, and reflect practical scenarios where users choose a safe batch size. *Dynamic* uses dynamic batch size control but disables node reordering. We compare these baselines with DGI,

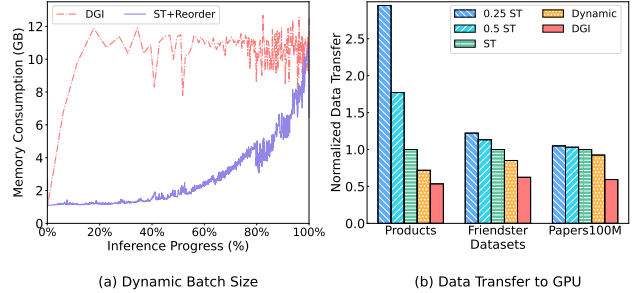


Figure 9. The effects of node reordering and dynamic batch size control. We use 3-layer GCN and the *Friendster* graph.

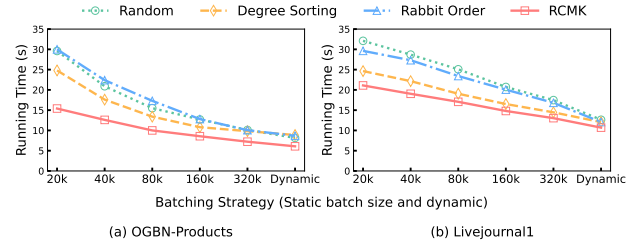


Figure 10. DGI using different node reordering methods. The experiments are conduct using 3-layer GCN on V100-16GB GPU.

which enables all optimizations.

Figure 11 reports the inference time of DGI and the baselines. The results show that *Dynamic* consistently outperforms *ST*, which indicates that dynamic batch size control is effective. To understand its benefit, we plot the GPU memory consumption for DGI and DGI without dynamic batch size control (denoted as *ST+Reorder*) in Figure 9(a). The results show that DGI fully utilizes GPU memory except for the initial bootstrap period. In contrast, static batch size (i.e., *ST+Reorder*) is limited by the memory consumption of the high degree nodes (in the last few batches) and thus has severe memory under-utilization. Figure 11 also shows that node reordering gives another performance boost to DGI (by comparing *Dynamic* with DGI). This is because node reordering organizes nodes with similar neighbors into the same batch to reduce the number of input neighbor embeddings. Figure 9(b) reports the data transfer for the baselines. The results show that node reordering enables DGI to save

up to 39.7% of the data traffic compared with Dynamic.

There are many methods to reorder nodes in a graph to improve cache locality, which share the same spirit with the RCMK-based node reordering in DGI. We compare RCMK with 3 alternatives: (i) *Random*, which randomly shuffles the nodes; (ii) *Degree Sorting*, which sorts the nodes by their in-degrees; (iii) Rabbit Order (Arai et al., 2016), which uses hierarchical community detection to determine node order. Figure 10 shows that RCMK consistently yields shorter inference time than the other methods, which justifies using RCMK in DGI. This is because RCMK uses BFS to assign node IDs, and nodes with adjacent IDs are likely to share input nodes. We conjecture that Rabbit Order has poor performance because focus on improve graph locality by storing neighbors in CPU caches (typically tens of MB) for graph algorithms like PageRank. Thus, it generates small neighborhood and is not suitable for GNN inference.

Hardware choices. Cloud providers (e.g., AWS, Azure and Alibaba) offer machine instances with different memory capacities and GPUs, and DGI can adapt to different instances by storing data in either SSD or main memory. Thus, an interesting question is how to select a proper machine instance to conduct GNN inference. We report such results in Table 5, which show that inference time significantly reduces when all data can be stored in main memory. Even if data does not fit in main memory, larger memory capacity still reduces inference time. Moreover, larger GPU memory is effective in reducing inference time. As advanced GPUs are very expensive on cloud, we suggest to ensure that the instance has enough main memory in the first place.

Table 5. Execution time of DGI (in seconds) on different machines. The models have 3 layers, and cases that store data on SSD are marked in bold. The first number is the capacity of main memory.

Machine	OGBN-Papers100M			Friendster		
	GCN	GAT	JKNet	GCN	GAT	JKNet
128 GB + 16 GB T4	1828	2840	2030	3070	4510	3220
192 GB + 16 GB T4	1590	2360	1730	2660	3930	3030
488 GB + 16 GB V100	509	1074	659	582	1290	801
1.5 TB + 32 GB V100	277	644	325	356	822	459

6 RELATED WORKS

Systems for GNN training. DGL (Wang et al., 2019) and PyTorch Geometric (PyG) (Fey & Lenssen, 2019) are state-of-the-art frameworks for GNN training. PyTorch-Direct (Min et al., 2021) and TorchQuiver (tor, 2021) train GNN on large graphs that exceed GPU memory by storing data on CPU memory and accessing them via CUDA unified virtual addressing (UVA). DistDGL (Zheng et al., 2020), Neugraph (Ma et al., 2019), Roc (Jia et al., 2020) and AliGraph (Yang, 2019) scale GNN training to multiple machines. These and many other systems (Wang et al.,

2020; Liu et al., 2020; Thorpe et al., 2021; Liu et al., 2021; Chen et al., 2020) are primarily designed for GNN training instead of inference.

Computation optimizations for GNN. GCNP (Zhou et al., 2021) computes node embedding efficiently by reducing the dimension of the intermediate embeddings. GNNAutoScale (Fey et al., 2021) uses the historical embeddings (i.e., computed in previous iterations) of neighbors to conduct aggregation. The two works trade accuracy for efficiency and are orthogonal to our DGI. PCGraph (Zhang et al., 2021) reduces data transfer overhead by caching node embeddings in GPU. Partition-based sparse matrix multiplication (SPMM) is used to run each layer of GNN models efficiently on FPGA (Zhang et al., 2020). These optimizations (i.e., embedding caching and layer execution) can also be integrated into DGI. To our knowledge, the idea of layer-wise inference is also seen in two code snippets (??), which however are manually written to handle simple GNN models with a linear structure only. We started the DGI project independently and our work formalizes the procedure of layer-wise inference, analyzes its advantages over node-wise inference, and we also design a system to make layer-wise inference general for GNN models and easy to use by translating the training code.

Currently, we assume that DGI works for a static graph. This scenario is observed in many applications that periodically update the graph structure, GNN model and node embedding (Ying et al., 2018; Liu et al., 2018). A challenging scenario is to update node embedding for dynamic graphs in real-time. In particular, the graph is receiving updates (e.g., edge insertion/deletion, node feature changes), node embedding needs to be updated accordingly for applications with high requirements on accuracy (e.g., recommendation and fraud detection). However, for an L -layer GNN model, a node/edge update can affect the embedding of its L -hop neighbors, which results in an enormous update set. Theory/algorithm may be required to limit the update set (e.g., skip a target node if changes to its embedding is smaller than a threshold in terms of Euclidean norm), and DGI can take the pruned update set as target nodes.

7 CONCLUSIONS

We build DGI, a system that makes inference easy and efficient for GNN models. We observe that the popular node-wise inference approach is inefficient and present a layer-wise inference approach, which is efficient but difficult to program. To mitigate such programming difficulty, DGI automatically traces the computation graph for GNN models, partitions the computation graph for execution, and manages node batching. DGI is general for different GNN models and inference requests, and supports out-of-core execution for large graphs.

A AN EXAMPLE OF HAND-WRITTEN LAYER-WISE INFERENCE FOR JKNET

```

1 # We adopt the forward function of JKNet from the DGL
2 # library, and implement layer-wise inference for JKNet
3 # manually.
4 class JKNet(nn.Module):
5     def __init__(...):
6         ... # init for JKNet.
7
8     def forward(self, g, x):
9         hs = []
10        h = x
11        for layer in self.layers:
12            h = layer(g, h)
13            h = self.dropout(h)
14            hs.append(h)
15        h = torch.cat(hs, dim=-1)
16        return self.conv(h)
17
18    def inference(self, g, batch_sizes, x):
19        feat_lst = []
20        for l, layer in enumerate(self.layers):
21            ret = torch.zeros(
22                (g.num_nodes(), self.hidden))
23            feat_lst.append(ret)
24            dl = NodeDataLoader(
25                batch_size=batch_sizes[0], ...)
26            for in_nodes, out_nodes, blocks in dataloader:
27                block = blocks[0].to("GPU")
28                h = x[in_nodes].to("GPU")
29                h = layer(block, h)
30                h = self.dropout(h)
31                feat_lst[-1][out_nodes] = h.cpu()
32            x = feat_lst[-1]
33
34        ret = torch.zeros(
35            (g.num_nodes(), self.n_classes))
36        dl = NodeDataLoader(
37            batch_size=batch_sizes[1], ...)
38        for in_nodes, out_nodes, blocks in dataloader:
39            block = blocks[0].to("GPU")
40            h_lst = []
41            for feat in feat_lst:
42                h_lst.append(feat[in_nodes].to("GPU"))
43            h = torch.cat(h_lst, dim=-1)
44            out_val = self.conv(h)
45            ret[out_nodes] = out_val.cpu()
46        return ret

```

Listing 1. Simplified handwritten code for the layer-wise inference of JKNet.

```

1 graph = ... # Graph data
2 x = ... # Node features
3 nids = torch.arange(graph.num_nodes())
4 model = JKNet(...)
5
6 # Inference by DGI.
7 from dgl.data import FullNeighborSampler
8 from dgi import AutoInferencer
9 infer = AutoInferencer(model,
10     targets=nids,
11     sampler=FullNeighborSampler(1),
12     computing_device="GPU:0",
13     external_device="CPU")
14 # Here takes the same arguments as
15 # forward function in JKNet.
16 pred = infer.inference(graph, x)

```

Listing 2. Code for using DGI for layer-wise inference of JKNet.

To demonstrate the challenges of coding layer-wise inference and the usability of DGI, Listing 1 shows how to use handwritten code to conduct layer-wise inference for JKNet.

For the forward function, JKNet first computes each layer’s embeddings and records them in an array. Finally, it concatenates all embeddings and uses an additional graph convolution to perform the output. It consists of only 8 LOCs (i.e., Line 8-16 in Listing 1) and node-wise influence is easy to implement by directly using the forward function. However, layer-wise inference needs approximately 30 LOCs (from Line 18 in Listing 1) even the code is already simplified by removing some of the complex and troublesome API calls. Line 20 first enumerates convolution layers, and performs layer-wise inference. For the additional graph convolution layer in JKNet, we need to write another layer-wise code for it (line 38 - 45). Note that the final layer of JKNet (i.e., the jumping knowledge layer) aggregates the output embedding of all preceding layers. The handwritten code needs to explicitly consider whether UVA memory is used in the CPU and manually configure the batch size for the dataloader. If data are stored on SSD, the handwritten code will be even more complex. Besides, the inference speed of layer-wise execution is sensitive to multiple factors such as the size of each node batch and the order to process nodes.

Listing 2 shows how to perform layer-wise inference using DGI. DGI provides an interface that users only need to input the model to initialize an *AutoInferencer*, which will automatically trace and split the forward function and pack it to the inference function. Then, users only need to call the inference function provided by *AutoInferencer*, which takes the arguments as the same as the model forward function. DGI completely frees the user from having to write all this tedious code.

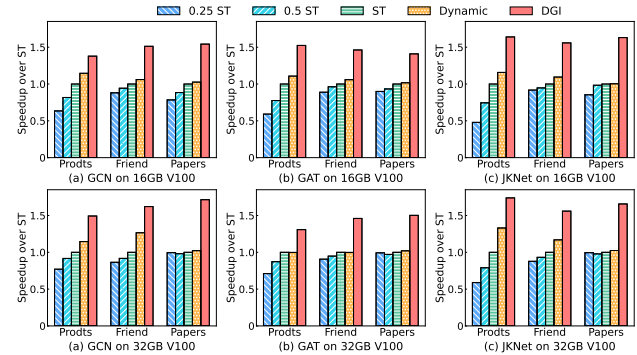


Figure 11. Speedup of dynamic batch size and node ordering in DGI over using the best static batch size found by profiling.

B MORE EXPERIMENTS COMPARING THE DGI VARIANTS

We compare the DGI variants (introduced in Figure 8 of the main paper) on the V100 GPU with 32GB memory in Figure 11. To observe the influence of GPU memory, we also include the results on the V100 GPU with 16GB memory

alongside. The results show that dynamic batch size and node ordering are effective for both GPU configurations—*Dynamic* performs close to or better than *ST*, and DGI significantly outperforms *Dynamic* with node ordering. The performance gap among different batch sizes (i.e., $0.25ST$, $0.5ST$ and ST) is smaller for 32GB GPU memory than 16GB GPU memory because 32GB memory allows larger batch sizes for all baselines and the gains of input sharing diminish with batch size.

REFERENCES

- Dgl code snippets. https://github.com/dmlc/dgl/blob/master/examples/pytorch/rgcn-hetero/entity_classify_mb.py, 2021.
- Quiver. <https://github.com/quiver-team/torch-quiver>, 2021.
- Exact code snippets. https://github.com/warai-0toko/Exact/blob/main/mem_speed_bench/models/sage.py, 2022.
- Arai, J., Shiokawa, H., Yamamuro, T., Onizuka, M., and Iwamura, S. Rabbit order: Just-in-time parallel reordering for fast graph analysis. In *2016 IEEE International Parallel and Distributed Processing Symposium (IPDPS)*, pp. 22–31. IEEE, 2016.
- Chan, W.-M. and George, A. A linear time implementation of the reverse cuthill-mckee algorithm. *BIT Numerical Mathematics*, 20(1):8–14, 1980.
- Chen, J., Ma, T., and Xiao, C. Fastgcn: Fast learning with graph convolutional networks via importance sampling. In *International Conference on Learning Representations*, 2018.
- Chen, Z., Yan, M., Zhu, M., Deng, L., Li, G., Li, S., and Xie, Y. fusegcn: accelerating graph convolutional neural network training on gpgpu. In *2020 IEEE/ACM International Conference On Computer Aided Design (ICCAD)*, pp. 1–9. IEEE, 2020.
- Cheung, M. and Moura, J. M. Graph neural networks for covid-19 drug discovery. In *IEEE International Conference on Big Data (Big Data)*, pp. 5646–5648. IEEE, 2020.
- Chiang, W.-L., Liu, X., Si, S., Li, Y., Bengio, S., and Hsieh, C.-J. Cluster-gcn: An efficient algorithm for training deep and large graph convolutional networks. In *Proceedings of the 25th ACM SIGKDD International Conference on Knowledge Discovery & Data Mining*, pp. 257–266, 2019.
- Fey, M. and Lenssen, J. E. Fast graph representation learning with PyTorch Geometric. In *ICLR Workshop on Representation Learning on Graphs and Manifolds*, 2019.
- Fey, M., Lenssen, J. E., Weichert, F., and Leskovec, J. Gnnautoscale: Scalable and expressive graph neural networks via historical embeddings. In *International Conference on Machine Learning*, pp. 3294–3304. PMLR, 2021.
- Gao, Y., Liu, Y., Zhang, H., Li, Z., Zhu, Y., Lin, H., and Yang, M. *Estimating GPU Memory Consumption of Deep Learning Models*, pp. 1342–1352. Association for Computing Machinery, New York, NY, USA, 2020. ISBN 9781450370431. URL <https://doi.org/10.1145/3368089.3417050>.
- Garcia Duran, A. and Niepert, M. Learning graph representations with embedding propagation. *Advances in neural information processing systems*, 30, 2017.
- Gaudelet, T., Day, B., Jamasb, A. R., Soman, J., Regep, C., Liu, G., Hayter, J. B., Vickers, R., Roberts, C., Tang, J., et al. Utilizing graph machine learning within drug discovery and development. *Briefings in bioinformatics*, 22(6):bbab159, 2021.
- Hamaguchi, T., Oiwa, H., Shimbo, M., and Matsumoto, Y. Knowledge transfer for out-of-knowledge-base entities: a graph neural network approach. In *Proceedings of the 26th International Joint Conference on Artificial Intelligence*, pp. 1802–1808, 2017.
- Hamilton, W. L., Ying, R., and Leskovec, J. Inductive representation learning on large graphs. In *Proceedings of the 31st International Conference on Neural Information Processing Systems, NIPS’17*, pp. 1025–1035, Red Hook, NY, USA, 2017. Curran Associates Inc. ISBN 9781510860964.
- Harris, C. R., Millman, K. J., Van Der Walt, S. J., Gommers, R., Virtanen, P., Cournapeau, D., Wieser, E., Taylor, J., Berg, S., Smith, N. J., et al. Array programming with numpy. *Nature*, 585(7825):357–362, 2020.
- Hu, W., Fey, M., Zitnik, M., Dong, Y., Ren, H., Liu, B., Catasta, M., and Leskovec, J. Open graph benchmark: Datasets for machine learning on graphs. *Advances in neural information processing systems*, 33:22118–22133, 2020a.
- Hu, Z., Dong, Y., Wang, K., and Sun, Y. Heterogeneous graph transformer. In *Proceedings of The Web Conference*, pp. 2704–2710, 2020b.
- Jia, Z., Lin, S., Gao, M., Zaharia, M., and Aiken, A. Improving the accuracy, scalability, and performance of graph neural networks with roc. *Proceedings of Machine Learning and Systems*, 2:187–198, 2020.

- Karypis, G. and Kumar, V. Metis: A software package for partitioning unstructured graphs, partitioning meshes, and computing fill-reducing orderings of sparse matrices. 1997.
- Kipf, T. N. and Welling, M. Semi-supervised classification with graph convolutional networks. In *International Conference on Learning Representations*, 2017.
- Klicpera, J., Bojchevski, A., and Günnemann, S. Predict then propagate: Graph neural networks meet personalized pagerank. In *International Conference on Learning Representations*, 2018.
- Kunegis, J. and Lommatzsch, A. Learning spectral graph transformations for link prediction. In *Proceedings of the 26th Annual International Conference on Machine Learning*, pp. 561–568, 2009.
- Liu, H., Lu, S., Chen, X., and He, B. G3: when graph neural networks meet parallel graph processing systems on gpus. *Proceedings of the VLDB Endowment*, 13(12): 2813–2816, 2020.
- Liu, T., Chen, Y., Li, D., Wu, C., Zhu, Y., He, J., Peng, Y., Chen, H., Chen, H., and Guo, C. Bgl: Gpu-efficient gnn training by optimizing graph data i/o and preprocessing. *arXiv preprint arXiv:2112.08541*, 2021.
- Liu, Z., Chen, C., Yang, X., Zhou, J., Li, X., and Song, L. Heterogeneous graph neural networks for malicious account detection. In *Proceedings of the 27th ACM International Conference on Information and Knowledge Management*, pp. 2077–2085, 2018.
- Ma, L., Yang, Z., Miao, Y., Xue, J., Wu, M., Zhou, L., and Dai, Y. {NeuGraph}: Parallel deep neural network computation on large graphs. In *2019 USENIX Annual Technical Conference (USENIX ATC 19)*, pp. 443–458, 2019.
- Mandal, S. and Maiti, A. Graph neural networks for heterogeneous trust based social recommendation. In *International Joint Conference on Neural Networks (IJCNN)*, pp. 1–8. IEEE, 2021.
- Min, S. W., Wu, K., Huang, S., Hidayetoğlu, M., Xiong, J., Ebrahimi, E., Chen, D., and Hwu, W.-m. Pytorch-direct: Enabling gpu centric data access for very large graph neural network training with irregular accesses. *arXiv preprint arXiv:2101.07956*, 2021.
- Riesen, K. and Bunke, H. *Graph classification and clustering based on vector space embedding*, volume 77. World Scientific, 2010.
- Sanders, P. and Schulz, C. Think locally, act globally: Highly balanced graph partitioning. In *International Symposium on Experimental Algorithms*, pp. 164–175. Springer, 2013.
- Schlichtkrull, M., Kipf, T. N., Bloem, P., Berg, R. v. d., Titov, I., and Welling, M. Modeling relational data with graph convolutional networks. In *European semantic web conference*, pp. 593–607. Springer, 2018.
- Thorpe, J., Qiao, Y., Eyolfson, J., Teng, S., Hu, G., Jia, Z., Wei, J., Vora, K., Netravali, R., Kim, M., et al. Dorylus: Affordable, scalable, and accurate {GNN} training with distributed {CPU} servers and serverless threads. In *15th USENIX Symposium on Operating Systems Design and Implementation (OSDI 21)*, pp. 495–514, 2021.
- Veličković, P., Cucurull, G., Casanova, A., Romero, A., Liò, P., and Bengio, Y. Graph attention networks. In *International Conference on Learning Representations*, 2018. URL <https://openreview.net/forum?id=rJXmpikCZ>.
- Wang, M., Zheng, D., Ye, Z., Gan, Q., Li, M., Song, X., Zhou, J., Ma, C., Yu, L., Gai, Y., Xiao, T., He, T., Karypis, G., Li, J., and Zhang, Z. Deep graph library: A graph-centric, highly-performant package for graph neural networks. *arXiv preprint arXiv:1909.01315*, 2019.
- Wang, Y., Feng, B., Li, G., Li, S., Deng, L., Xie, Y., and Ding, Y. Gnnadvisor: An adaptive and efficient runtime system for gnn acceleration on gpus. *arXiv preprint arXiv:2006.06608*, 2020.
- Wang, Z., Chen, T., Ren, J. S., Yu, W., Cheng, H., and Lin, L. Deep reasoning with knowledge graph for social relationship understanding. In *Proceedings of the 26th International Joint Conference on Artificial Intelligence*, 2018.
- Wei, L., Zhao, H., and He, Z. Designing the topology of graph neural networks: A novel feature fusion perspective. In *Proceedings of the ACM Web Conference 2022*, pp. 1381–1391, 2022.
- Xu, K., Li, C., Tian, Y., Sonobe, T., Kawarabayashi, K.-i., and Jegelka, S. Representation learning on graphs with jumping knowledge networks. In *International Conference on Machine Learning*, pp. 5453–5462. PMLR, 2018.
- Yang, H. Aligraph: A comprehensive graph neural network platform. In *Proceedings of the 25th ACM SIGKDD international conference on knowledge discovery & data mining*, pp. 3165–3166, 2019.
- Yang, J. and Leskovec, J. Defining and evaluating network communities based on ground-truth. *Knowledge and Information Systems*, 42(1):181–213, 2015.

- Ying, R., He, R., Chen, K., Eksombatchai, P., Hamilton, W. L., and Leskovec, J. Graph convolutional neural networks for web-scale recommender systems. In *Proceedings of the 24th ACM SIGKDD international conference on knowledge discovery & data mining*, pp. 974–983, 2018.
- Zhang, B., Zeng, H., and Prasanna, V. Hardware acceleration of large scale gcn inference. In *2020 IEEE 31st International Conference on Application-specific Systems, Architectures and Processors (ASAP)*, pp. 61–68. IEEE, 2020.
- Zhang, L., Lai, Z., Tang, Y., Li, D., Liu, F., and Luo, X. Pc-graph: Accelerating gnn inference on large graphs via partition caching. In *2021 IEEE Intl Conf on Parallel & Distributed Processing with Applications, Big Data & Cloud Computing, Sustainable Computing & Communications, Social Computing & Networking (ISPA/BDCloud/Social-Com/SustainCom)*, pp. 279–287. IEEE, 2021.
- Zhang, M. and Chen, Y. Link prediction based on graph neural networks. *Advances in neural information processing systems*, 31, 2018.
- Zheng, D., Ma, C., Wang, M., Zhou, J., Su, Q., Song, X., Gan, Q., Zhang, Z., and Karypis, G. Distdgl: distributed graph neural network training for billion-scale graphs. In *2020 IEEE/ACM 10th Workshop on Irregular Applications: Architectures and Algorithms (IA3)*, pp. 36–44. IEEE, 2020.
- Zhou, H., Srivastava, A., Zeng, H., Kannan, R., and Prasanna, V. Accelerating large scale real-time gnn inference using channel pruning. *arXiv preprint arXiv:2105.04528*, 2021.